Heavy quark diffusion in an overoccupied gluon plasma

J. Peuron[a,*]

[a]*Dept. of Astronomy and Theoretical Physics, Sölvegatan 14A, S-223 62 Lund, Sweden*

E-mail: jarkko.peuron@thep.lu.se

We extract the heavy quark diffusion coefficient κ and the resulting momentum broadening $\langle p^2 \rangle$ of a heavy quark embedded in a far-from-equilibrium gluon plasma using classical-statistical lattice simulations. We find several features in the time dependence of the momentum broadening: a short initial rapid growth of $\langle p^2 \rangle$, followed by linear growth with time due to Langevin-type dynamics and damped oscillations around this growth at the plasmon frequency. We show that these novel oscillations are not easily explained using perturbative techniques but result from an excess of gluons at low momenta. These oscillation are therefore a gauge invariant confirmation of the infrared enhancement we had previously observed in gauge-fixed correlation functions. We argue that the kinetic theory description of such systems becomes less reliable in the presence of this IR enhancement.
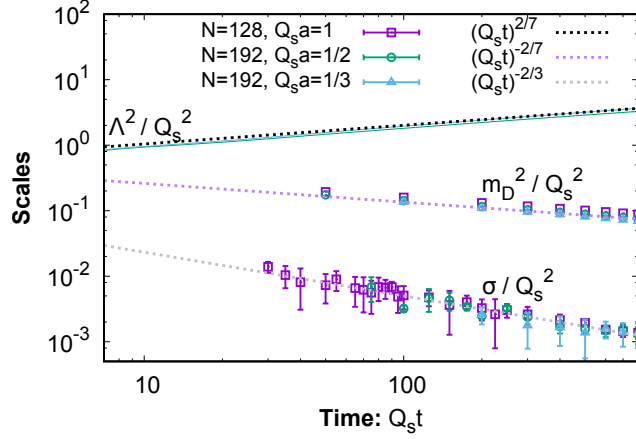
---

[*]Speaker

Figure 1: An example of hierarchy of scales generated in a classical field simulation in the self-similar regime. Fig. originally from [8].

1. Introduction

In the early stages of an ultrarelativistic heavy-ion collision gluon fields with nonperturbatively large phase-space occupation numbers at the characteristic momentum scale Q_s are generated [1]. This overoccupied system of gluons becomes effectively classical and can therefore be studied using real time lattice simulations. In this work we study the heavy quark momentum diffusion coefficient during the initial glasma stage in a non-expanding system. Our aim is to understand how important the initial nonequilibrium evolution is for the heavy quark momentum diffusion coefficient κ. Recently nonequilibrium transport coefficients in overoccupied systems have been studied in e.g. [2–6].

We are working in the limit of large quark mass. This permits us to tremendously simplify the extraction procedure using the heavy quark as a test particle. In this approach we need to only measure the forces that the medium would exert on the quark. Hence, computationally more costly fermion simulations can be replaced by cheaper pure glue simulations.

Classical gluodynamical systems, along with scalar field theory, are known to exhibit non-thermal fixed points and self-similar scaling [7]. Effectively this means that at late times the dynamics of the system are greatly simplified and many properties follow simple power laws. This leads into emergence of similar hierarchy of scales as in thermal field theory in the Hard Thermal Loop framework. Therefore, this framework can predict certain features of the gluodynamical systems far from equilibrium. This dynamically generated hierarchy of scales is illustrated in Fig. 1 [8].

This paper presents a compact summary of our work on this topic. For a more detailed and comprehensive overview we refer the reader to [9]. All figures shown in this paper are from [9], except Fig. 1, which is from [8].
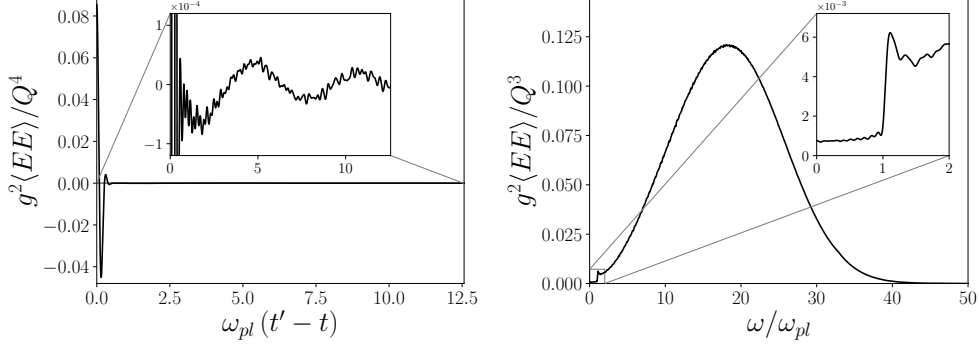
Figure 2: The plot on the LHS shows the unequal time electric field correlation function in the time domain, and the RHS plot shows the correlation function in the frequency domain. The large initial correlation in the time domain corresponds to the broad peak in the frequency domain with $\omega \gg \omega_{pl}$. The oscillations in the time domain with the frequency ω_{pl} correspond to the kink at ω_{pl} in the frequency domain.

2. Heavy quark in a color field

On the classical level a heavy quark embedded in the glasma obeys the classical equation of motion

$$\dot{p}_i(t) = \mathcal{F}_i(t) \,. \tag{1}$$

The chromoelectric force $\mathcal{F}_i$ has no preferred direction $\langle \dot{p} \rangle = 0$ but a nonzero variance

$$\langle \dot{p}_i(t) \dot{p}_i(t') \rangle = \frac{g^2}{N_c} \text{Tr} \langle E_i(t) U_0(t, t') E_i(t') U_0(t', t) \rangle = \frac{g^2}{2N_c} \langle EE \rangle (t, t'). \tag{2}$$

In (2) the temporal links are eliminated by choosing temporal gauge, as is commonly done in real time lattice simulations. The unequal time force-force correlation function is shown in both time and frequency domains in Fig. 2. The correlator has two distinct features: initial rapidly decaying large correlation, and the following considerably weaker oscillatory correlation. In the frequency domain the sharp rise in the correlation at $\omega = \omega_{pl}$ arises from the quasiparticle (QP) contribution, and the intercept with the y-axis $\approx \kappa$ is given by the Landau damping of longitudinal gluon fields. This effect will be discussed in more detail in Sec. 3.

2.1 Momentum broadening

The force-force correlation function given by (2) also predicts the momentum broadening of a heavy quark embedded in the glasma. Integrating the unequal time correlation function over time we obtain the average momentum broadening between t and $t + \Delta t$

$$\langle p^2(t, \Delta t) \rangle = \frac{g^2}{2N_c} \int_t^{t+\Delta t} dt' \int_t^{t+\Delta t} dt'' \, \langle EE \rangle (t', t'') \,. \tag{3}$$

A numerical extraction is shown in Fig. 3. We observe that the broadening has 3 distinct features. At the timescale given by the hard scale Λ, $\Delta t \approx 2\pi/\Lambda$, the broad peak in Fig. 2 dominates the integration, resulting in a sharp rise in momentum broadening. This is followed by a stage
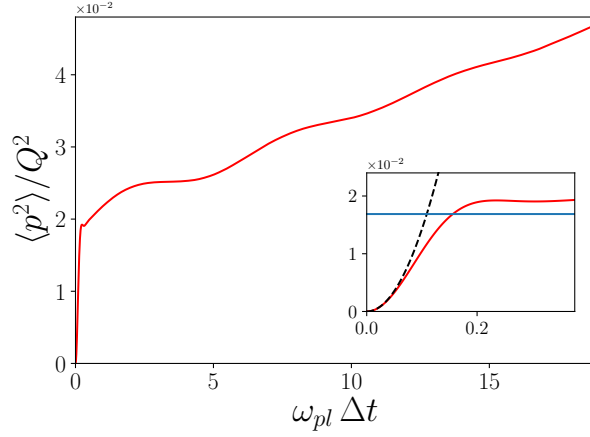
Figure 3: Momentum broadening extracted from a numerical simulation in dimensionless time scaled to the units of the plasma frequency ω_{pl}.

characterized by approximately linear growth in Δt in the region $1/\Lambda \ll \Delta t \ll t$. This is consistent with a Langevin description. On top of the linear growth we observe damped oscillations with period $\Delta t \approx 2\pi/\omega_{pl}$. These oscillations arise from transverse quasiparticle excitations. The oscillations will be discussed in more detail in Sec. 3.

2.2 Momentum broadening & heavy quark diffusion

In order to connect momentum broadening to the diffusion coefficient κ, we define $\kappa(t, \Delta t)$ as

$$3\kappa (t, \Delta t) = \frac{\mathrm{d}}{\mathrm{d}\Delta t} \langle p^2 (t, \Delta t) \rangle \tag{4}$$

As in thermal equilibrium, the diffusion coefficient $\kappa(t)$ is defined at $\Delta t \to \infty$ limit

$$\frac{g^2}{2N_c} \langle EE \rangle (t, \omega = 0) = 3\,\kappa_\infty(t)\,. \tag{5}$$

On the lattice $\kappa(t, \Delta t)$ is given by

$$\kappa (t, \Delta t) \approx \frac{g^2}{3N_c} \int_t^{t+\Delta t} \mathrm{d}t' \int \frac{\mathrm{d}^3 x}{V} \langle E_i^a(t, \mathbf{x}) E_i^a(t', \mathbf{x}) \rangle, \tag{6}$$

To identify $\kappa(t, \Delta t) = \kappa(t)$ we want to have $t \gg \Delta t \gg 1/\gamma_{pl}$, where $1/\gamma_{pl}$ is the largest inverse lifetime of QP excitations. This quantity has been measured in real time lattice simulations for far from equilibrium gluon plasma in [10].

2.2.1 Understanding the Δt dependence in $\kappa(t, \Delta t)$

Our numerical evaluation of $\kappa(t, \Delta t)$ is shown in Fig. 4. We observe that $\kappa(t, \Delta t)$ oscillates in Δt with the frequency ω_{pl}, which in the self-similar regime scales as

$$\omega_{pl}^2 = \frac{4}{3}N_c \int \frac{\mathrm{d}^3 p}{(2\pi)^3} \frac{g^2 f(t, p)}{\omega(p)} \sim t^{-2/7}. \tag{7}$$
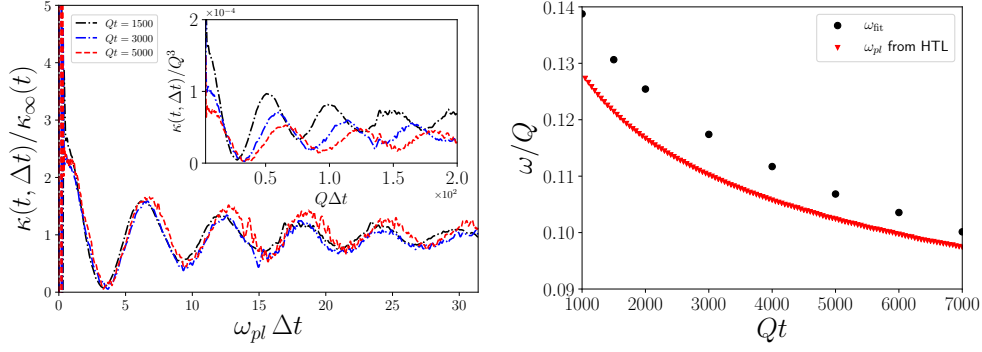
Figure 4: LHS: Lattice extraction of $\kappa(t, \Delta t)$. The inset shows the x- and y-axis without any rescaling. RHS: Here we show the frequency extracted from $\kappa(t, \Delta t)$ in Δt using damped oscillator fit, and the plasmon frequency extracted using (7). We observe that they agree to 10% level.

In Fig. 4 the x-axis is scaled by ω_{pl} and the y-axis is scaled by the infinity value $\kappa(t, \Delta t \to \infty)$ corresponding to the diffusion coefficient. We observe that the curves fall very nicely on top of each other, indicating that ω_{pl} is the right scaling variable for the frequency. The inset in Fig. 4 shows $\kappa(t, \Delta t)$ without the rescaling. The diffusion coefficient is extracted by performing a damped oscillator fit to the signal. Furthermore, right hand panel of Fig. 4 also shows the extracted oscillation frequency of $\kappa(t, \Delta t)$ in Δt (which is also obtained from the fit) and is in agreement with the frequency extracted from (7).

3. Spectral Reconstruction (SR) method

To relate our measurements to the distribution of gluons as measured from equal-time electric field correlators, we have constructed a parametrization that we refer to as the spectral reconstruction. In order to understand the oscillations in $\kappa(t, \Delta t)$ we start from (6) and write $\kappa(t, \Delta t)$ as

$$3\kappa(t, \Delta t) = \frac{g^2}{N_c} \int_{-\infty}^{\infty} \frac{d\omega}{2\pi} \frac{\sin(\omega \Delta t)}{\omega} \int \frac{d^3 p}{(2\pi)^3} \langle EE \rangle(t, \omega, p). \tag{8}$$

The Fourier transform of the EE correlation function $\langle EE \rangle(t, \omega, p)$ can be expressed in terms of spectral (ρ) and statistical ($\langle EE \rangle(t, t, p)$) correlation functions using the generalized fluctuation-dissipation relation [10]

$$\langle EE \rangle_{T,L}(t, \omega, p) = \frac{\dot{\rho}(t, \omega, p)}{\dot{\rho}(t, t, p)} \langle EE \rangle_{T,L}(t, t, p). \tag{9}$$

$$\dot{\rho}(\omega, p) = 2\Im\mathfrak{m} G_R^{\text{HTL}}(\omega, p), \tag{10}$$

The retarded propagator $G_R^{\text{HTL}}(\omega, p)$ can be evaluated in perturbation theory in a straightforward manner. It consists of quasiparticle contributions which only contribute for $\omega \geq \omega_{pl}$ and Landau damping contributions for $\omega \leq \omega_{pl}$ in both transverse and longitudinal directions. The explicit expressions used here can be found in [9].

We will utilize our nonperturbative extraction of the quasiparticle dispersion $\omega(p)$ and the quasiparticle damping rate $\gamma(p)$ in our numerical framework, since they slightly differ from the
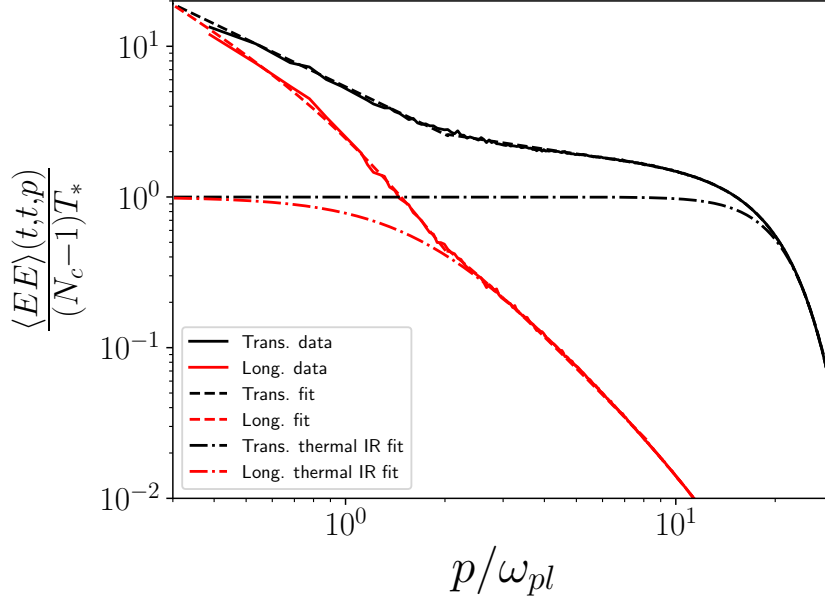
Figure 5: The extracted statistical correlation function and its thermal counterpart which has been matched to the numerical extraction in the large p region. This is a gauge dependent quantity, and the extraction is done in temporal gauge ($A^0 = 0 \ \forall t$). At readout times we also impose the Coulomb gauge condition $\nabla \cdot \boldsymbol{A}(t) = 0$.

equilibrium counterparts [10]. The statistical correlation function far-from equilibrium is considerably enhanced compared to its hard thermal loop theory counterpart in the infrared. The thermal expectation in HTL theory is $\langle EE \rangle_T \approx T_*$, corresponding to the quasiparticle spectrum $f(p) \approx \dfrac{T_*}{\sqrt{m^2 + p^2}}$. Far-from equilibrium we observe $\langle EE \rangle_T \gg T_*$ in the infrared. The extracted correlation function is shown in Fig. 5. Since the two are considerably different we will use parametrizations of both in our numerical framework. HTL perturbation theory does not predict the behavior of this correlation function for large p. Thus we regulate the thermal behavior by matching the thermal curve to the numerical curve in the large p region in order to make sure that the differences in the both approaches arise entirely from the differences in the IR region.

By making use of the fluctuation-dissipation relation, and the HTL retarded propagator discussed above, we can estimate the large t behavior of (8). At the $\Delta t \to \infty$ limit only longitudinal Landau damping contributes. Using the thermal IR assumption (with a step function cutoff at $p = \Lambda$) we get

$$\kappa^{\mathrm{SR}}_{\infty, LL}(t) \approx \frac{N_c^2 - 1}{12\pi N_c} m_D^2(t) g^2 T_*(t) \log\left(\frac{\Lambda(t)}{m_D(t)}\right) \sim (Qt)^{-5/7} \log(Qt). \tag{11}$$

This will be our expectation for the time dependence of $\kappa(t)$.

3.1 Understanding the oscillations in $\kappa(t, \Delta t)$

Our numerical evaluation of $\kappa(t, \Delta t)$ is compared to the SR parametrization in Fig. 6. The black curve corresponds to the unequal time correlation functions given by (6). For the spectral
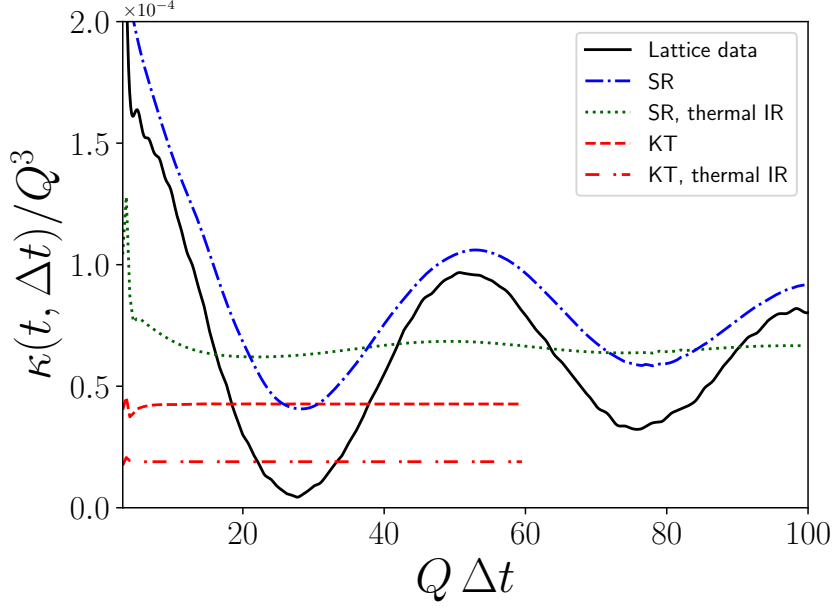
Figure 6: Numerical extraction of $\kappa(Qt = 1500, \Delta t)$ in Δt. The SR framework is discussed in Sec. 3 and the lattice extraction is given by (6).

reconstruction framework discussed in Sec. 3 we have two curves. One of them uses the thermal infrared assumption for the equal time electric field correlation function, and the other one uses the numerically extracted correlator. We also see a curve labeled as "KT" which is obtained by deriving a kinetic theory estimate for κ and using the quasiparticle distribution extracted from a real time lattice simulation as an input. We will not discuss the details of this method in this proceeding and refer the reader to [9] for the details of the procedure. For a more comprehensive description of kinetic theory extraction we refer the reader to [11].

    We observe that the oscillations in $\kappa(t, \Delta t)$ which are observed when the diffusion coefficient is extracted using (6) are only reproduced when the infrared enhancement of the equal time correlation function is taken into account in the spectral reconstruction method. Furthermore, the spectral reconstruction framework can be broken down into transverse and longitudinal quasiparticle and Landau damping contributions. The frequency of the oscillations in the IR enhanced spectral reconstruction curve arises from the transverse quasiparticle modes, and the offset from the x-axis arises from the longitudinal Landau damping. Since $\kappa(t, \Delta t)$ is gauge invariant, we take this as a confirmation of the IR enhancement, which we already observed in the case of gauge fixed equal time correlation functions in Fig. 5.

3.2 Time evolution of $\kappa(t)$

    Finally, we want to study the time-evolution of the heavy quark momentum diffusion coefficient $\kappa(t)$. The numerical results are shown in Fig. 7. We use the functional form of (11) as a fit and observe that both methods nicely follow the expected behavior.
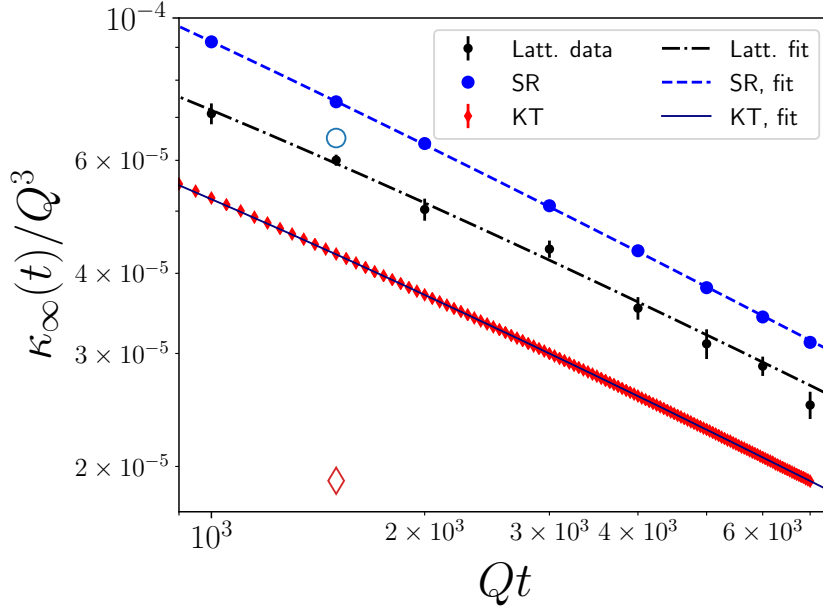
Figure 7: The extracted diffusion coefficient κ as a function of time t. Open symbols correspond to thermal infrared assumption and the closed symbols are using the numerically extracted equal time electric field correlation function. Data are shown by points and fits are shown by dashed lines.

4. Conclusions

In this work we have the extracted heavy quark momentum diffusion coefficient κ, and observed that its time-evolution is consistent with $\kappa \sim t^{-5/7} \log(t)$, which was predicted by HTL and self-similarity. We have also studied equal time electric field correlators, and found out that the nonequilibrium correlation function is enhanced in the infrared compared to the thermal case. This turns out to result into interesting oscillations in $\langle p^2 \rangle(\Delta t)$ and $\kappa(\Delta t)$ with frequency ω_{pl}. Thus we conclude that heavy quarks, quarkonia and jets may be sensitive to the infrared dynamics of nonequilibrium QGP.

Our future plans involve extracting transport coefficients during the hydrodynamization process. More specifically our current aim is to extract κ using effective kinetic theory during the bottom-up thermalization scenario.

Acknowledgments

References

[1] F. Gelis, *Initial state and thermalization in the color glass condensate framework*, *Int. J. Mod. Phys.* **E24** (2015) no. 10 1530008 [`arXiv:1508.07974 [hep-ph]`].

[2] A. Ipp, D. I. Müller and D. Schuh, *Jet momentum broadening in the pre-equilibrium Glasma*, *Phys. Lett. B* **810** (2020) 135810 [`arXiv:2009.14206 [hep-ph]`].

[3] A. Ipp, D. I. Müller and D. Schuh, *Anisotropic momentum broadening in the 2+1D Glasma: analytic weak field approximation and lattice simulations*, `arXiv:2001.10001 [hep-ph]`.

[4] M. E. Carrington, A. Czajka and S. Mrowczynski, *Heavy quarks embedded in glasma*, `arXiv:2001.05074 [nucl-th]`.

[5] Y. Sun, G. Coci, S. K. Das, S. Plumari, M. Ruggieri and V. Greco, *Impact of Glasma on heavy quark observables in nucleus-nucleus collisions at LHC*, *Phys. Lett.* **B798** (2019) 134933 [`arXiv:1902.06254 [nucl-th]`].

[6] S. Mrowczynski, *Heavy quarks in turbulent QCD plasmas*, *Eur. Phys. J.* **A54** (2018) no. 3 43 [`arXiv:1706.03127 [nucl-th]`].

[7] J. Berges, K. Boguslavski, S. Schlichting and R. Venugopalan, *Universal attractor in a highly occupied non Abelian plasma*, *Phys. Rev.* **D89** (2014) 114007 [`arXiv:1311.3005 [hep-ph]`].

[8] M. Mace, S. Schlichting and R. Venugopalan, *Off-equilibrium sphaleron transitions in the glasma*, *Phys. Rev.* **D93** (2016) 074036 [`arXiv:1601.07342 [hep-ph]`].

[9] K. Boguslavski, A. Kurkela, T. Lappi and J. Peuron, *Heavy quark diffusion in an overoccupied gluon plasma*, *JHEP* **09** (2020) 077 [`arXiv:2005.02418 [hep-ph]`].

[10] K. Boguslavski, A. Kurkela, T. Lappi and J. Peuron, *Spectral function for overoccupied gluodynamics from real-time lattice simulations*, *Phys. Rev.* **D98** (2018) no. 1 014006 [`arXiv:1804.01966 [hep-ph]`].

[11] G. D. Moore and D. Teaney, *How much do heavy quarks thermalize in a heavy ion collision?*, *Phys. Rev.* **C71** (2005) 064904 [`arXiv:hep-ph/0412346 [hep-ph]`].